NANO LETTERS

2007
Vol. 7, No. 6
1785−1788

Predictive Study of Charge Transport in Disordered Semiconducting Polymers

Stavros Athanasopoulos,[†] James Kirkpatrick,[‡] Diego Martínez,[†] Jarvist M. Frost,[‡] Clare M. Foden,[§] Alison B. Walker,*[,†] and Jenny Nelson[‡]

Department of Physics, University of Bath, Bath BA2 7AY, United Kingdom, Department of Physics, Imperial College London, London SW7 2BW, United Kingdom, and CDT Oxford Ltd., Greenwich House, Madingley Rise, Madingley Road, Cambridge CB3 0TX, United Kingdom

Received April 13, 2007; Revised Manuscript Received May 9, 2007

ABSTRACT

We present a theoretical study of charge transport in disordered semiconducting polymers that relates the charge mobility to the chemical structure and the physical morphology in a novel multiscale approach. Our studies, focusing on poly(9,9-dioctylfluorene) (PFO), show that the charge mobility is dominated by pathways with the highest interchain charge-transfer rates. We also find that disorder is not always detrimental to charge transport. We find good agreement with experimental time-of-flight mobility data in highly aligned PFO films.

The use of disordered organic semiconductors such as π conjugated polymers (CPs) for displays, energy efficient lighting, solar cells, sensors, and thin film transistors is of intense interest due to their flexibility, light weight, and the potential for low manufacturing costs.[1] A fundamental limitation is the low value of electron and hole mobilities, μ_e and μ_h, typically in the range $10^{-7}-10^{-3}$ cm^2/(Vs). Subtle changes in chain packing can have a strong effect on the value of mobility. Important factors are the degree of alignment of polymer backbones,[2] thermally induced crystallization,[3] and influence of side-chain length[4,5] and molecular weight[6,7] on polymer chain conformation. It is clear that major improvements in device performance could be made if the polymer film morphology could be controlled and optimized. Thus an understanding of how morphology influences mobility will have significant technological implications. There is a strong need for robust theories of the electronic properties of molecular nanomaterials in order to fully exploit their potential applications, and the relationship between electronic properties and morphology is also highly relevant for a wide range of nanomaterial systems including inorganic nanoparticle assemblies and bioelectronic systems as well as organic semiconductors.[8,9]

Fundamental interest arises from the difficulty in predicting electrical transport properties of disordered molecular solids from the chemical structure. The challenge lies in the fact that, in CPs, the local packing of chains determines microscopic charge-transfer rates and the formation of conduction pathways on longer length scales. Simulating realistic disordered morphologies on such multiple length scales is extremely hard. Even once a morphology is known, efficient ways of calculating microscopic charge transport parameters and of simulating the charge dynamics must be available in order to obtain a value for the mobility.

In this paper, we address the influence of weak disorder on hole mobility, μ_h, in films of aligned polymer chains. We focus on poly-(9,9′-dioctylfluorene) (PFO), a blue-emitting CP of practical interest for light emission that has one of the highest μ_h yet reported for a CP ($\mu_h \sim 10^{-3}-10^{-2}$ cm^2/Vs).[2,3] The material adopts ordered configurations in certain conditions and the relationship between processing, morphology, and the resulting optical[10] and transport[2,3] properties has been well characterized experimentally. Here, we introduce a protocol for charge transport modeling, which incorporates the effects of chemical structure, through quantum chemical calculations of the electronic transfer rates, and structural disorder, through random variations in molecular position and orientation that are sampled using kinetic Monte Carlo (MC) simulations of hopping under an applied electric field.

Until now, hopping transport in disordered molecular films has commonly been analyzed within the context of the Gaussian disorder model (GDM)[11] and its variants. The GDM provides an expression for the temperature and electric field dependence of μ_h in terms of disorder in transport site energies and in hopping rates. This empirical formalism was obtained using MC simulations of a biased random walk (RW) on disordered cubic lattices, normally using a Miller−Abrahams (MA) intersite hopping rate. Although the GDM has been used for comparative analysis of experimental data, it offers no way to predict charge-transport properties from

* Corresponding author. E-mail: a.b.walker@bath.ac.uk.
† Department of Physics, University of Bath.
‡ Department of Physics, Imperial College London.
§ CDT Oxford Ltd.

10.1021/nl0708718 CCC: $37.00
Published on Web 05/24/2007

the physical and chemical structure of real molecular materials because the MA rate parameters cannot be calculated directly from chemical structure and because no details of the positions of charge transport units are included.

Our method also uses MC simulations of a biased RW to model charge transport but it overcomes the limitations of the GDM by, first, employing an arrangement of charge transporting units that is based on the observed structure of the crystalline PFO material and, second, using small-polaron hopping rates calculated directly from the electronic structure of the units. We use nonadiabatic Marcus−Hush theory[12] for the intermolecular hole transfer rate, Γ,

$$\Gamma_{ij} = \frac{2\pi}{\hbar} J_{ij}^{\,2} \frac{1}{\sqrt{4\pi\lambda k_B T}} \exp\left\{ - \frac{(\Delta G_{ij} - \lambda)^2}{4\lambda k_B T} \right\} \qquad (1)$$

where J_{ij} is the electronic transfer integral, λ is the molecular reorganization energy (equal to half the polaron binding energy), ΔG_{ij} is the free energy difference between initial and final sites, k_B is Boltzmann's constant, and T the temperature. This expression was also used in refs 3,13,14 in calculations of μ_h for pentacene stacks and simple models of CPs. Thus, through calculation of electronic properties from first principles using an empirical morphology, our method can disentangle the influences of morphology and chemical structure on mobility.

We model a film of aligned PFO chains as a hexagonal lattice of lattice constant a where the chains are parallel both to each other and to the substrate, following X-ray diffraction studies.[15] A trimer of fluorene with a length of 2.3 nm is the charge transporting unit in all cases: the trimer is the oligomer of length closest to the spatial extent of polarons in other polymers (2.0 nm for polythiophene,[16] 2.5 nm for PPV[17]). Charge transporting units in CPs are expected to be of varying length and may vary dynamically in position and size through thermal fluctuations. Here, we restrict attention to a static lattice and to the case of trimers only, in order to focus on the effects of positional and torsional disorder, without invoking energetic disorder due to varying segment length. The relaxed geometry of the trimer is calculated in Gaussian 03[18] using density functional theory (DFT) with the B3LYP hybrid functional and Pople's double-ζ split basis set with added polarization functions 6-31 g*; all trimers are assumed to take this geometry in the neutral state.

The trimers are arranged coaxially in columns, aligned with the z direction, as a model of a continuous chain. The trimer position is determined by the midpoint of the trimer relative to the (x,y) axes and the torsion angle, ϕ, by the angle between the plane of the central fluorene unit and the $x-z$ plane. The simulation cell consists of 20×20 chains, where each chain consists of 10 trimers and periodic boundary conditions are applied in the x and y directions. The morphology model and degrees of freedom are shown in Figure 1. We consider the following cases: (i) an ordered morphology, where all trimers are located on lattice points with the same torsion angle ϕ; (ii) a torsionally disordered system, where ϕ is distributed at random in the range $0-2\pi$;

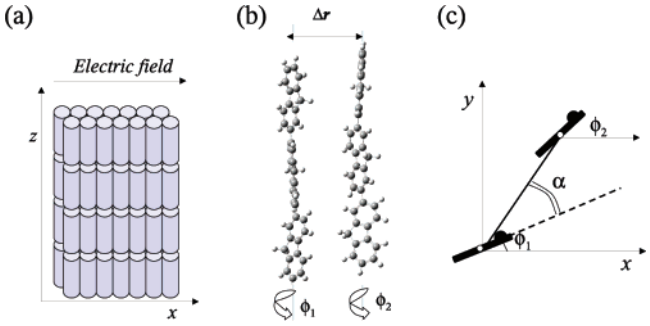

Figure 1. (a) Model morphology for aligned polymer chains. Each column contains trimers stacked end-to-end. (b) A pair of neighboring PFO trimers (C atoms are indicated by dark spheres and H atoms by light spheres) showing interchain separation $\Delta\mathbf{r}$ and torsion angles ϕ. The octyl side chains are replaced by H atoms for the calculation of J and λ. (c) Top view of the central planes of two trimers, showing the torsion angles ϕ_1 and ϕ_2 ($\Delta\phi = \phi_2 - \phi_1$) and the polar angle α.

(iii) a regular system (called the optimally ordered case), where relative torsion angles are chosen to maximize the net transfer rate in the field direction. Lateral disorder is simulated via random lateral trimer displacements in the $x-y$ plane taken from a uniform distribution, with a minimum separation of 0.63 nm to allow for excluded volume. The hopping transport parameters are calculated as follows: λ takes the internal reorganization energy value of 0.204 eV calculated from the method in ref 19. An additional contribution due to external reorganization is neglected here because its value is poorly defined. $\Delta G_{ij} = e\Delta\mathbf{r_{ij}}\cdot\mathbf{F}$, where $\Delta\mathbf{r_{ij}}$ joins the midpoints of initial and final trimers, $\mathbf{F}$ is the applied electric field, and e is the magnitude of the electron charge. There is no contribution to ΔG_{ij} due to differences in the trimer HOMO levels because all transport units are rigid copies of the same relaxed geometry (i.e., there is no variation in HOMO energy due to molecular conformation) and electrostatic interactions between the molecules are expected to be weak in this system and are therefore neglected.

Because of the large number of possible relative orientations to be sampled, a computationally efficient method is needed to calculate J. We calculate the molecular orbitals (MOs) of an isolated trimer using the intermediate neglect of differential overlap Hamiltonian with Zerner's parametrization for spectroscopic applications (ZINDO/S). J is obtained using a simplification of the ZINDO/S Hamiltonian, which does not require self-consistent field calculations on each pair of molecules.[20] For hops between trimers in the same chain, we ignore the terminal H atom and assume trimers are separated by the bond length between fluorene units in the polymer. Although this is a crude model of intrachain transport, the mobility is insensitive to intrachain hop rates provided they exceed interchain rates by a factor of at least 100.

A MC transport simulation is executed on the chosen morphology as follows. For a charge on site i, a waiting time τ_{ij} is calculated for a hop from site i to each of its six interchain and two intrachain nearest neighbor sites, j: $\tau_{ij} = -\ln(X)/\Gamma_{ij}$, where X is a random number uniformly distributed between 0 and 1. The hop with the smallest waiting

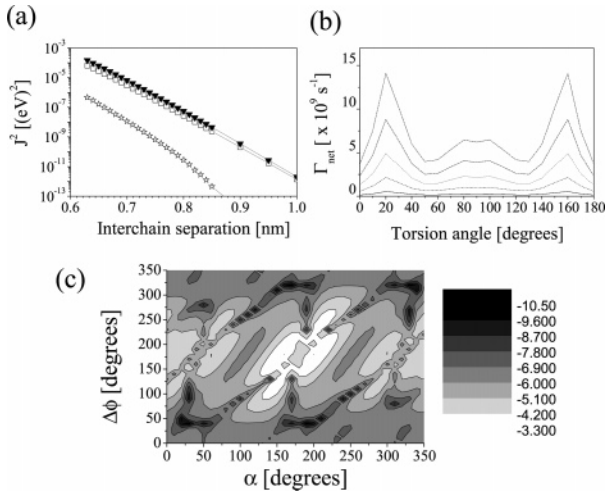

Figure 2. (a) J^2 vs $|\Delta\mathbf{r}|$ for $\alpha = 0$, $\Delta\phi = 0$ (☆); $\alpha = 0$, $\Delta\phi = 150°$ (□); $\alpha = 60°$, $\Delta\phi = 180°$ (▼). (b) Γ_{net} for a forward hop along the x direction in an ordered system as a function of ϕ for $a = 0.65$ nm and, in increasing order of size, of Γ_{net}, $\sqrt{F} = 200$, 400, 600, 800, 1000 $(V/cm)^{1/2}$. (c) Contour plot of $J^2(\Delta\phi,\alpha)$ for $|\Delta\mathbf{r}| = 0.65$ nm. The numbers shown in the legend are $\log_{10}(J^2)$.

time is chosen, and the hop executed and the simulation time is advanced by τ_{ij}. We follow the trajectory of a hole randomly placed on a trimer in the film and calculate the time for the hole to travel a fixed distance d, typically 10 cell widths in the field direction. A transit time averaged over several hundred trajectories, $\langle\tau\rangle$, is obtained. The field-dependent mobility μ is computed from $\mu = d/(\langle\tau\rangle F)$. Simulations of μ gave similar results in cells of 1000 nm in width.

J^2 is sensitive to chain separation $|\Delta\mathbf{r}|$ and relative orientation $\Delta\phi,\alpha$. Figure 2a shows that variations of only 0.25 nm in $|\Delta\mathbf{r}|$ result in relative changes of $\sim 10^5$ in J^2. For systems with little disorder in chain positions at low fields, μ_h will be dominated by the sum, Γ_{net}, of the hopping rates Γ_{ij} to nearest neighbor j of site i, weighted by the relative step length in the field direction. This sum is plotted in Figure 2b, where it can be seen that the most favorable torsion angle is $\phi = 20°$ for $\mathbf{F}$ directed along the x axis; therefore, this value of ϕ is used for our ordered morphology. Figure 2c shows that J^2 is low when the π systems are parallel (ordered systems have $\Delta\phi = 0$) and is higher, for example, when $150° < \Delta\phi < 210°$. Therefore an optimally ordered morphology was chosen where neighboring trimers in the x direction have $\Delta\phi = 150°$.

In Figure 3, we present the simulated mobility for several morphologies in the Poole−Frenkel ($\log \mu$ versus $F^{1/2}$) representation widely used for experimental mobility data. We focus on the case of $a = 0.65$ nm, with $\mathbf{F}$ directed along the x axis. Interestingly, the torsionally disordered system leads to a μ_h approximately 10 times larger than the ordered case with fixed $\phi = 20°$. Introducing lateral disorder had little effect on the μ_h of the torsionally disordered system at this chain separation. Likewise, the effect of disorder in slip has little effect on the torsionally disordered case, as can be understood from our fast interchain transfer rates. It is at first surprising that μ_h for the torsionally disordered system

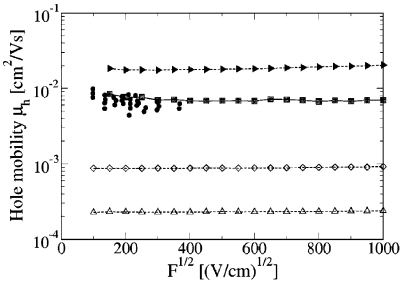

Figure 3. Poole−Frenkel plot for predicted μ_h compared to experimental data[2,3] (●) in an aligned PFO film at $T = 300$ K, an interchain separation $a = 0.65$ nm, where $\mathbf{F}\|x$. Predicted μ_h values are shown for the ordered system devised to maximize μ_h (filled right triangles), the ordered system with fixed $\phi = 20°$ (◊), with fixed $\phi = 0°$ (Δ), and a lateral and torsionally disordered system (■). The lines are to guide the eye.

exceeds that of an ordered system where ϕ is constant. The comparison between the disordered and ordered cases can be understood from Figure 2c, which shows that the highest values of J^2 occur for molecular orientations where the trimers are not parallel. In a torsionally disordered system, "sweet spots" will be sampled where the interchain transfer rate is much higher than in the ordered case. Pathways for fast charge transport can then be formed, linking these sweet spots, similar to the concept of charge highways in disordered materials.[21] An optimally ordered morphology designed to exploit these sweet spots is also shown on Figure 3. By allowing the unit cell more than one trimer, such that $\Delta\phi$ between the different elements of the unit cell is nonzero (specifically, $\Delta\phi = 150°$ for nearest neighbors along the $+x$ direction and $\Delta\phi = 180°$ for $\alpha = 60°$), an ordered system has been devised for which the resulting μ_h is even higher than the randomly disordered morphology.

Also shown on Figure 3 are experimental data for a film of PFO where polymer chains have been aligned parallel to each other and to the substrate.[3,2] No particular torsional alignment is expected for this material. The field dependence and magnitude of the experimental data are well reproduced by the torsionally disordered simulation for $a \approx 0.65$ nm. The value $a \approx 0.9$ nm from a nominal density of 1 g cm^{-3} results in much reduced transfer rates for a torsionally disordered system (see Figure 2a). Our model is unlikely to underestimate the transfer rates because we have already neglected the outer-sphere contribution to the reorganization energy. Furthermore, the overall film density is unlikely to be very much larger than the nominal value. However, the film may contain domains with varying chain densities, such that charges are transported more easily through the denser domains. Because the interchain J^2 is so strongly dependent on chain separation while intrachain J^2 remains relatively high, transport will be rate-limited by the fastest interchain hops. In a system where chains are sufficiently flexible to come into contact occasionally, such hops will occur at the smallest possible interchain separation, which we find to be 0.63 nm for octyl side chains. Therefore, it is not surprising that the experimental μ_h is reproduced by a model where the fastest interchain hops are characteristic of the distance of closest approach of PFO chains. To test this, we have

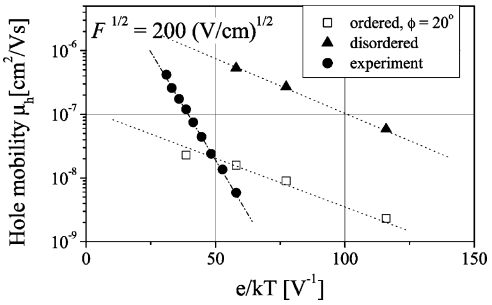

Figure 4. Simulated μ_h vs inverse temperature compared to experimental data[3] (●) for an annealed PFO film, at $\sqrt{F} = 200$ (V/cm)$^{1/2}$.

simulated transport in a torsionally and laterally disordered system with $a = 0.9$ nm with sufficient lateral disorder for neighboring trimers to come within 0.63 nm of each other. We find that μ_h is reduced by $\sim 10^3$ relative to the disordered system with $x = 0.65$ nm and the same distance of closest approach, while J^2 falls by $\sim 10^5$ over the same range of a. Thus, the interchain hopping points or "sweet spots" appear to be the critical determinants of charge transport.

Studies by Chen and co-workers using transmission electron microscopy and X-ray diffraction[5] suggest that the unit cell of PFO may have a more complex structure than the simple hexagonal model suggested by Kawana and co-workers.[15] The shortest interchain distance in the unit cell they predict is approximately 0.6 nm. This value is close to the chain separation used for the simulation of the torsionally disordered system in Figure 3, which agreed well with experiment, and suggests that transport in PFO is rate-limited by hops between chains at a relative separation of at least 0.6 nm.

Finally, we address energetic disorder, which has not been included in the model. Figure 4 shows the T dependence of μ_h at $\sqrt{F} = 200$ (V/cm)$^{1/2}$ for the ordered case with fixed $\phi = 20°$, the torsionally disordered case, and the experimental data for annealed (not aligned) PFO from ref 3. The similarity of the ordered and disordered cases is expected from the low field limit of eq 1, where the weak T dependence (the activation energy $E_a \approx 40$ meV) results from the low value of λ used. The neglected contribution to λ due to external reorganization will be of a similar size so the much stronger T dependence ($E_a \approx 150$ meV) of the experimental data is likely to result in part from disorder in the hole site energies due both to variations in the conjugated segment length and electrostatic interchain interactions. These effects will be incorporated in a more refined model.

In conclusion, we have simulated charge transport in fluorene-based polymer films using a method that includes explicitly the chemical structure and morphology of the polymer. Our technique goes beyond the Gaussian disorder model and lattice Monte Carlo techniques. The method is quite general and can be applied to other molecular systems of different morphologies and levels of disorder. A key conclusion is that the points of closest electronic contact between chains rate-limit charge transport, with the result that positional disorder in polymer chains can even increase mobility. One implication of this is that high mobility may be achievable in dilute blends provided that polymer chains are sufficiently stretched and in contact. Such behavior has recently been observed experimentally in thiophene polymer blends.[22]

Acknowledgment. This work is supported in part by the UK Engineering and Physical Sciences Research Council, the Royal Society, Cambridge Display Technology, and the European Commission STREP project MODECOM (NMP-CT-2006-016434).

References

(1) Marks, P. *New Scientist* **2007**, *2588*, 24.
(2) Redecker, M.; Bradley, D. D. C.; Inbasekaran, M.; Woo, E. P. *Appl. Phys. Lett.* **1999**, *74*, 1400.
(3) Kreouzis, T.; Poplavskyy, D.; Tuladhar, S. M.; Campoy-Quiles, M.; Nelson, J.; Campbell, A. J.; Bradley, D. D. C. *Phys. Rev. B* **2006**, *73*, 235201.
(4) Martens, H. C. F.; Blom, P. W. M.; Schoo, H. F. M. *Phys. Rev. B* **2000**, *61*, 7489.
(5) Chen, S. H.; Chou, H. L.; Su, A. C.; Chen, S. A. *Macromolecules* **2004**, *37*, 6833.
(6) Inigo, A. R.; Tan, C. H.; Fann, W.; Huang, Y.-S.; Perng, G.-Y.; Chen, S.-A. *Adv. Mater.* **2001**, *13*, 504.
(7) Kline, R. J.; McGehee, M. D.; Toney, M. F. *Nat. Mater.* **2006**, *5*, 222.
(8) Watkins, P. K.; Walker, A. B.; Verschoor, G. L. B. *Nano Lett.* **2005**, *5*, 1814.
(9) Frost, J. M.; Cheynis, F.; Tuladhar, S. M.; Nelson, J. *Nano Lett.* **2006**, *6*, 1674.
(10) Campoy-Quiles, M.; Etchegoin, P. G.; Bradley, D. D. C. *Phys. Rev. B* **2005**, *72*, 045209.
(11) Bässler, H. *Phys. Status Solidi B* **1993**, *175*, 15.
(12) Brédas, J.-L.; Beljonne, D.; Coropceanu, V.; Cornil, J. *Chem. Rev.* **2004**, *104*, 4971.
(13) Olivier, Y.; Lemaur, V.; Brédas, J.-L.; Cornil, J. *J. Phys. Chem. A* **2006**, *110*, 6356.
(14) Chatten, A. J.; Tuladhar, S. M.; Choulis, S. A.; Bradley, D. D. C.; Nelson, J. *J. Mater. Sci.* **2005**, *40*, 1393.
(15) Kawana, S.; Durrell, M.; Lu, J.; Macdonald, J. E.; Grell, M.; Bradley, D. D. C.; Jukes, P. C.; Jones, R. A. L.; Bennett, S. L. *Polymer* **2002**, *43*, 1907.
(16) Knupfer, M.; Fink, J.; Fichou, D. *Phys. Rev. B* **2001**, *63*, 165203.
(17) Shimoi, Y.; Abe, S.; Kuroda, S.; Murata, K. *Solid State Commun.* **1995**, *95*, 137.
(18) Frisch, M. J.; Trucks, G. W.; Schlegel, H. B.; Scuseria, G. E.; Robb, M. A.; Cheeseman, J. R.; Montgomery, J. A., Jr.; Vreven, T.; Kudin, K. N.; Burant, J. C.; Millam, J. M.; Iyengar, S. S.; Tomasi, J.; Barone, V.; Mennucci, B.; Cossi, M.; Scalmani, G.; Rega, N.; Petersson, G. A.; Nakatsuji, H.; Hada, M.; Ehara, M.; Toyota, K.; Fukuda, R.; Hasegawa, J.; Ishida, M.; Nakajima, T.; Honda, Y.; Kitao, O.; Nakai, H.; Klene, M.; Li, X.; Knox, J. E.; Hratchian, H. P.; Cross, J. B.; Bakken, V.; Adamo, C.; Jaramillo, J.; Gomperts, R.; Stratmann, R. E.; Yazyev, O.; Austin, A. J.; Cammi, R.; Pomelli, C.; Ochterski, J. W.; Ayala, P. Y.; Morokuma, K.; Voth, G. A.; Salvador, P.; Dannenberg, J. J.; Zakrzewski, V. G.; Dapprich, S.; Daniels, A. D.; Strain, M. C.; Farkas, O.; Malick, D. K.; Rabuck, A. D.; Raghavachari, K.; Foresman, J. B.; Ortiz, J. V.; Cui, Q.; Baboul, A. G.; Clifford, S.; Cioslowski, J.; Stefanov, B. B.; Liu, G.; Liashenko, A.; Piskorz, P.; Komaromi, I.; Martin, R. L.; Fox, D. J.; Keith, T.; Al-Laham, M. A.; Peng, C. Y.; Nanayakkara, A.; Challacombe, M.; Gill, P. M. W.; Johnson, B.; Chen, W.; Wong, M. W.; Gonzalez, C.; Pople, J. A. *Gaussian 03*, revision C.02; Gaussian, Inc.: Wallingford, CT, 2004.
(19) Sakanoue, K.; Motoda, M.; Sugimoto, M.; Sakaki, S. *J. Phys. Chem. A* **1999**, *103*, 5551.
(20) Kirkpatrick, J. *Int. J. Quantum Chem.* **2007**, DOI: 10.1002/qua.21378.
(21) Borsenberger, P. M.; Pautmeier, L.; Bässler, H. *J. Chem. Phys.* **1991**, *94*, 5447.
(22) Goffri, S.; Müller, C.; Stingelin-Stutzmann, N.; Breiby, D. W.; Radano, C. P.; Andreasen, J. W.; Thompson, R.; Janssen, R. A. J.; Nielsen, M. M.; Smith, P.; Sirringhaus, H. *Nat. Mater.* **2006**, *5*, 950.

NL0708718